Received: 29 August 2023 | Accepted: 14 November 2023

DOI: 10.1111/jpy.13417

RESEARCH ARTICLE

Elemental and macromolecular plasticity of *Chlamydomonas reinhardtii* (Chlorophyta) in response to resource limitation and growth rate

Jana Isanta-Navarro | **Logan M. Peoples** | **Benedicta Bras** | **Matthew J. Church** | **James J. Elser**

Flathead Lake Biological Station, University of Montana, Polson, Montana, USA

Correspondence
Jana Isanta-Navarro, Flathead Lake Biological Station, University of Montana, 32125 Bio Station Lane, Polson, MT, USA.
Email: jana.isanta-navarro@bio.ku.dk

Present address
Jana Isanta-Navarro, Department of Biology, University of Copenhagen, Copenhagen, Denmark

Funding information
National Science Foundation, Grant/Award Number: DEB-1930816

Editor: X. Johnson

Abstract

With the ongoing differential disruption of the biogeochemical cycles of major elements that are essential for all life (carbon, nitrogen, and phosphorus), organisms are increasingly faced with a heterogenous supply of these elements in nature. Given that photosynthetic primary producers form the base of aquatic food webs, impacts of changed elemental supply on these organisms are particularly important. One way that phytoplankton cope with the differential availability of nutrients is through physiological changes, resulting in plasticity in macromolecular and elemental biomass composition. Here, we assessed how the green alga *Chlamydomonas reinhardtii* adjusts its macromolecular (e.g., carbohydrates, lipids, and proteins) and elemental (C, N, and P) biomass pools in response to changes in growth rate and the modification of resources (nutrients and light). We observed that *Chlamydomonas* exhibits considerable plasticity in elemental composition (e.g., molar ratios ranging from 124 to 971 for C:P, 4.5 to 25.9 for C:N, and 15.1 to 61.2 for N:P) under all tested conditions, pointing to the adaptive potential of *Chlamydomonas* in a changing environment. Exposure to low light modified the elemental and macromolecular composition of cells differently than limitation by nutrients. These observed differences, with potential consequences for higher trophic levels, included smaller cells, shifts in C:N and C:P ratios (due to proportionally greater N and P contents), and differential allocation of C among macromolecular pools (proportionally more lipids than carbohydrates) with different energetic value. However, substantial pools of N and P remained unaccounted for, especially at fast growth, indicating accumulation of N and P in forms we did not measure.

KEYWORDS
carbon, chemostat, Chlamydomonas, energy, green algae, growth rate hypothesis, nitrogen, phosphorus, stoichiometry

Abbreviations: ATP, adenosine triphosphate; C, carbon; EDTA, ethylenediaminetetraacetic acid; GRH, growth rate hypothesis; N, nitrogen; NADPH, nicotinamide adenine dinucleotide phosphate; P, phosphorus; RNase, ribonuclease.

INTRODUCTION

The elements carbon (C), nitrogen (N), and phosphorus (P) are key nutrients for all life. In the Anthropocene, biogeochemical cycles of these bioelements have been drastically and differentially altered, disrupting processes from organismal to ecosystem levels (Dudgeon, 2019; Melack, 2016; Peñuelas et al., 2013; Sardans et al., 2012; Vitousek et al., 1997). Understanding these disruptions is facilitated by the emergence of the field of ecological stoichiometry, the study of the balance of energy and multiple chemical elements in ecological interactions (Sterner & Elser, 2002). Knowledge of variation in C:N:P ratios is important for understanding a variety of ecological and ecosystem processes (e.g., competition, trophic interactions, and nutrient recycling), and given the differential disruptions in major nutrient supplies in the Anthropocene, this knowledge becomes increasingly important. To survive and reproduce, organisms must contend with these differential disruptions. An important ability that allows organisms to cope with environmental heterogeneity or temporal fluctuations is phenotypic plasticity (De Jong, 2005; Fusco & Minelli, 2010).

Phenotypic plasticity can be defined as the ability of individual genotypes to develop different phenotypes when exposed to different environmental conditions (Pigliucci, 2006). Specific environmental cues thereby lead to physiological shifts within developmental-based constraints (West-Eberhard, 2003), resulting in individuals with altered phenotypic states or activities (e.g., metabolism; Garland & Kelly, 2006). Plastic responses of an organism not only have consequences for the organism itself, but plasticity can also improve fitness, enabling proliferation under changing environmental conditions. Such shifts can also have consequences for the organism's consumers. For example, development of high C:P ratios in primary producer biomass can impose food quality constraints on consumers, while changes in the N:P ratio of algae biomass can alter the rates and ratios at which N and P are recycled by consumers (Caron et al., 1985; Sterner & Elser, 2002; Weers & Gulati, 1997).

While supplies of C, N, and P vary naturally in aquatic ecosystems in space and time (Lampert & Sommer, 2007), anthropogenic impacts increasingly intensify or differentially (i.e., in different directions or degrees) alter resource availability. The C:N:P ratios of algae reflect their macromolecular composition (e.g., protein, carbohydrate, lipid, nucleic acids, and pigments) and can respond strongly to environmental variation (Geider & La Roche, 2002; Sterner & Elser, 2002). The phylogenetic diversity of macromolecular composition in algae has been studied, and it is known that groups and species of phytoplankton can be distinct in their biomass composition (Finkel et al., 2016; Martiny et al., 2013). However, knowledge about within-species or within-strain variation is more limited, although various individual macromolecular and elemental pools have been studied in response to different environmental limitations. However, a comprehensive assessment of a broad suite of major biochemical pools in conjunction with assessment of C:N:P stoichiometry under differing environmental conditions and growth rates has not been conducted.

Here, we document the phenotypic plasticity of elemental and macromolecular composition within a single genotype of a green algae, *Chlamydomonas reinhardtii*, a model organism widely used across a broad range of studies in biology. Previous studies of the compositional plasticity of *C. reinhardtii* have focused on assessing individual elemental or macromolecular pools but have not included a full spectrum of components as we have here. Most studies have focused on shifts in C:N:P stoichiometry driven by temperature or irradiance. Based on these studies, we know that *C. reinhardtii* N:P ratios decrease with increasing irradiance (Thrane et al., 2016), that higher temperatures lead to higher N:P ratios (Thrane et al., 2017), and that P-limitation appears to be a major determinant of growth rate and cellular elemental stoichiometry (Hessen et al., 2017).

To test the hypotheses that growth rate and the identity of the limiting resource affect macromolecular and elemental composition, we examined how *Chlamydomonas reinhardtii* partitions C, N, and P among major macromolecular pools under four contrasting resource supply conditions and at different growth rates. Specifically, *C. reinhardtii* was grown in chemostats at growth rates of 20% and 80% of maximum growth rate (μ_{max}) under differing resource conditions (Low Light, Low N:P, High N:P, and Balanced N:P). Based on existing and emerging literature encapsulated in the growth rate hypothesis (GRH) and related stoichiometric approaches (Elser et al., 2000; Sterner & Elser, 2002), we predicted lower cell contents of the limiting resource in slow-dilution chemostats and, due to increased allocation to P-rich ribosomal RNA, lower N:P ratios in fast-growing cultures. We observed plastic responses to growth rate and the identity of the limiting resource across all treatments with implications for key concepts of ecological stoichiometry.

MATERIALS AND METHODS

Culture conditions

The green alga *Chlamydomonas reinhardtii* (CC-1690 wild-type mt + [Sager 21 gr], *Chlamydomonas* Resource Center, University of Minnesota, United States) was cultivated in COMBO medium (Kilham et al., 1998), a defined freshwater culture medium for algae and zooplankton that contains sodium bicarbonate. The stock

cultures were grown under constant light with no dark phase to minimize possible heterotrophic growth. *Chlamydomonas reinhardtii* was precultured in batch mode at 20°C and at a light intensity of ~100 μmol photons $\cdot m^{-2} \cdot s^{-1}$ (Philips F40T12/DX 40 Watts).

For the experiment, *Chlamydomonas reinhardtii* was grown continuously in 450-mL chemostats at 20°C and aerated with CO_2-enriched air (2%–3% CO_2). Quadruplicate chemostats were used for each of four different experimental treatments (three different N:P nutrient ratios and light intensity; Table 1). N:P ratios ranged from 6:1 (low N supply) to 16:1 (Redfield ratio, can be thought of as a "control" or "reference" treatment under saturating light conditions) to 80:1 (low P supply). Although most lake ecosystems are P-limited, seasonal variation in nutrient fluxes often leads to N-limitation or a co-limitation of both nutrients (Elser et al., 1990; Lampert & Sommer, 2007). The chosen ratios are within the range of N:P that occurs in natural systems around the world (Sterner & Elser, 2002). Chemostats were operated under constant light (LED panels from Viparspectra, model number P1000) with full spectrum light. The pH was monitored on a daily basis throughout the experiment and consistently remained at a value of ~7.

For all experiments, cells were grown in COMBO medium (Kilham et al., 1998) with changes in the media N:P ratios made by adjusting concentrations of $NaNO_3$ (see Table 1). Continuous dilution with fresh medium was controlled by a peristaltic pump. In steady-state chemostats, including light-limited chemostats, the cells are maintained at a constant, specific growth rate that is imposed by the dilution rate (Huisman et al., 2002). Hence, chemostats allow the experimenter to control the rate of growth independently from changes in the environment (e.g., temperature, media composition, and light). At steady state, the specific growth rate equals the dilution rate, following this equation:

$$\mu\left(d^{-1}\right) = \frac{f\left(d^{-1}\right)}{V}$$

where f is the dilution volume and V is the volume of the chemostat. In chemostats, the concentration of the limiting resource determines the cell density at equilibrium, but not the growth rate; for more information on chemostat theory, see Novick and Szilard (1950) and Smith and Waltman (1995). All treatments were run at 20% ($\mu = 0.5 \cdot d^{-1}$) and 80% ($\mu = 2.0 \cdot d^{-1}$) of the empirically determined maximum growth rate (~$2.5 \cdot d^{-1}$ based on chemostat wash-out rates). Samples for biochemical and biomolecular analysis were taken after 4–5 generations (2–4 days depending on growth rate) after reaching steady state. For sampling, the entire culture was removed from the chemostat and immediately processed for the analyses described below.

TABLE 1 Environmental conditions (nutrient and light limitation). The balanced treatment can be considered as a reference or control treatment, where light is in sufficient supply and the nutrient molar ratio follows the Redfield ratio.

Treatment	Light intensity (μmol photons $\cdot m^{-2} \cdot s^{-1}$)	Media N:P (molar ratio)
High N:P	200	80:1
Low N:P	200	6:1
Low Light	60	16:1
Balanced N:P	200	16:1

Determination of cell dry weight, cell count, and chlorophyll

For the determination of cell dry weight, 3–5 mL of the cultures were harvested and filtered onto preweighed Isopore™ polycarbonate membrane filters (0.2 μm, 25 mm). Filters with cell material were dried for at least 2 h in a drying oven at 105°C. After cooling to room temperature in a desiccator, filters were reweighed.

To determine cell abundances, 1 mL of culture was fixed with a final concentration of 3% formaldehyde overnight at 4°C. Cells were filtered onto 25-mm 0.2-μm GTTP filters and frozen at –20°C. DNA was stained using DAPI Vectashield (Vector Laboratories), and cells were visualized using an epifluorescence microscope (Olympus BX53). Cell counts were obtained by imaging cells based on chlorophyll autofluorescence using a TRITC excitation filter set. At least 10 fields of view or 200 cells were counted per sample. For cell length and width, ~1000 cells (at least 30 per sample) were manually quantified. *Chlamydomonas reinhardtii* cells are unevenly shaped (avocado-like) and the width is not consistent across the entire length. We therefore took the width at half the length of the cell. The length and width were used to estimate cell volume based on the assumption that the cell was an ellipsoid: however, cell shape changed depending on treament and growth state.

For the determination of concentrations of chlorophyll *a* (referred to as chlorophyll in the following), 1 mL of culture was filtered in the dark onto a glass microfiber filter (GF/F filter, Whatman, nominal pore size 0.7 μm, 25 mm). Filters were placed into 15-mL polypropylene centrifuge tubes and frozen overnight at –20°C, after which 10 mL of 90% acetone were added and samples were vortexed and stored at 4°C in the dark for 7 days to extract passively. After extraction, tubes containing the filters were centrifuged for 40 min at 2000 × *g* at 20°C (Allega X-14R Centrifuge, Beckman Coulter). Chlorophyll concentrations of the extracts were estimated based on fluorescence (10-AU Fluorometer, Turner Designs) and included an acid correction (Holm-Hansen et al., 1965).

Determination of protein, ATP, lipid, and carbohydrate

Total protein quantification of algal biomass was adapted from Wagner et al. (2015) using the Thermo Scientific™ Coomassie Plus™ Kit. A set of protein standards was prepared following the manufacturer protocol (Thermo Scientific) with the concentration of standards ranging from 25 to 2000 $\mu g \cdot mL^{-1}$. Protein was quantified using dried cell material. For these assays, 14 mL of lyophilized *Chlamydomonas reinhardtii* were homogenized in 400 µL 30% trichloroacetic acid (TCA), incubated at 4°C for 30 min, and then centrifuged at 15,500 *g* (4°C) for 10 min. The supernatant was removed and the pellet was rinsed with 400 µL of 5% TCA. After vortexing and centrifuging, the supernatant was removed, and 300 µL of 0.2 M sodium hydroxide (NaOH) was added to each tube. Samples were vortexed, and 50 µL of each sample or standard were added to 1.5 mL of Coomassie Plus Reagent (Thermo Scientific). Samples, and standards were mixed and incubated for 10 min at room temperature. A UV–Vis spectrophotometer (Agilent Cary 60) was used for colorimetric absorption (at 595 nm) analyses.

Adnosine triphosphate concentrations were determined based on quantifying bioluminescence resulting from the luciferase-catalyzed reaction of luciferin and ATP (Holm-Hansen, 1973). Briefly, 100 µL of culture were mixed with an equal volume of BacTiter-Glo reagent (Promega) and incubated in the dark at room temperature for 5 min. Luminescence was quantified using a luminometer (GloMax 20/20, Promega). ATP concentrations were calculated based on serial dilutions of a 1 µmoL $ATP \cdot L^{-1}$ primary standard (Sigma).

Total lipid content was analyzed by homogenizing 14 mL of lyophilized *Chalmydomonas reinhardtii* in 2:1 chloroform:methanol (v/v). Extraction followed the microsulfophosphovanillin method as developed by Gardner et al. (1985) and validated by Lu et al. (2008) and Wagner et al. (2015). Standards were prepared by dissolving cholesterol in 2:1 chloroform:methanol (v/v). Samples and standards were read on a spectrophotometer at 525 nm.

Carbohydrate was determined using methods previously described (Van Wychen et al., 2017; Van Wychen & Laurens, 2016). Briefly, 10 mL of *Chlamydomonas reinhardtii* culture was freeze-dried and stored at −80°C. Cell pellets were treated with 72% sulfuric acid and incubated at room temperature for 1 h with vortexing every 5–10 min. MilliQ-purified water (7 mL) was added to bring the concentration of sulfuric acid to 4%. Samples were placed into glass tubes with rubber-stoppers, crimped-sealed, and autoclaved for 1 h at 121°C. Samples were cooled to room temperature and centrifuged for 5 min at 4300 × *g*. Supernatant (50 µL) was transferred to a new tube and diluted 1:10 with MilliQ water to a final volume of 500 µL, to which 500 µL of 0.5 M NaOH and 500 µL MBTH working solution (1 $mg \cdot mL^{-1}$ DTT and 3 $mg \cdot mL^{-1}$ MBTH at 1:1 v/v) were added and the entire solution was incubated at 80°C for 15 min. Samples were immediately treated with 1 mL of ferric solution (0.25 M HCl with 0.5% ferric ammonium sulfate dodecahydrate and 0.5% sulfamic acid), vortexed, and incubated at room temperature for 15 min. Finally, samples were diluted with 2.5 mL of MilliQ water to bring the final volume to 5 mL. Absorbance was measured at 620 nm and carbohydrate concentrations were calculated using a standard curve created with dextrose (Sigma-Aldrich).

Determination of nucleic acids

DNA and RNA were quantified fluorometrically using protocols described in Gorokhova and Kyle (2002) and Kyle et al. (2003) using the Quant-iT RiboGreen RNA Reagent and Kit (Thermo Scientific). Briefly, 1 mL of culture was centrifuged at 23,500 *g* for 10 min at 4°C. Supernatant was discarded, and the cell pellet was frozen at −80°C until analyses. Pellets were resuspended in 300 µL of extraction buffer (1% N-lauroysarcosine in 1× TE buffer), sonicated on ice for 2 min, and incubated for 2 h with shaking at room temperature. Samples were diluted 1:6 with ice-cold TE buffer and shaken again for 15 min. DNA and RNA standards were prepared following the manufacturer protocols (Thermo Scientific) corresponding to 2 $\mu g \cdot mL^{-1}$ DNA or RNA, respectively. Samples and standards (75 µL) were aliquoted into black microplates, amended with 75 µL RiboGreen (Quant-iT™ RiboGreen RNA Reagent and Kit) and incubated for 5 min in the dark. Fluorescence was measured at 485/30 nm excitation and 528/20 emission on a microplate reader (FLx800 Bio-Tek). Each well was then amended with 10 µL of RNase (Promega) and incubated in the dark for 25 min to remove RNA. Fluorescence was measured again, and RNA and DNA were concentrations were calculated based on the difference in the two fluorescence measurements.

Determination of biomass C, N, and P

For analysis of biomass P, 5 mL of culture were filtered onto precombusted and acid-washed GF/F filters (Whatman), dried at 105°C overnight, and stored in a desiccator. Filters were placed in a scintillation vial, combusted at 500°C for 5 h, and then hydrolyzed with 10 mL 0.15 M HCl. Samples were analyzed colorimetrically on a spectrophotometer (880 nm, Agilent Cary 60 UV–Vis Spectrophotometer) following the molybdate method (Karl et al., 1991). Zooplankton and tomato leaves of known P contents were used as reference standards to evaluate P recovery. The amount of P in each sample was calculated based on the observed

concentration in the hydrolyzed sample and the volume of hydrolysate and converted to percent dry mass based on dry weight determination as described below.

For analysis of particulate C and N, 20 mL of culture were filtered onto precombusted GF/F filters (Whatman), dried at 105°C overnight, and stored in a desiccator. Carbon and N in each sample were determined using an Exeter CE440 Elemental Analyzer. Detailed protocols for elemental analysis can be found on the Flathead Lake Biological Station (FLBS) Public Data Portal (https://flbs.umt.edu/PublicData). EDTA was used as a calibration standard (EDTA LCRM Certified Reference Material Cat.# 60-00-4), and algae reference standards (*Spirulina* Standard 30 g Model B2162) were analyzed every 10 samples. Blank samples (filter and instrument blanks) were run at the beginning of the analysis to ensure no contamination from the environment inside the instrument after every 10 samples.

Conversion to contents

Elemental and biochemical data were converted to elemental and biochemical contents as percentage of dry mass by dividing volumetric concentrations of the measured macromolecules and elements by the volume-normalized dry weights for each sample and multiplying by 100.

Statistical analysis

Statistical analyses of elemental and macromolecular pools in *Chlamydomonas reinhardtii* under different resource limitations and growth rates were performed using SigmaPlot (Systat Software, version 14.0.). All data sets passed a normality test (Shapiro–Wilk) and equal variance test (Brown–Forsythe) prior to further analysis. To test for statistically significant differences, a two-way ANOVA with the factors resource limitation and growth rate was performed (File S1 in the Supporting Information), followed by pairwise multiple comparison tests (Tukey's HSD) of all treatments.

RESULTS AND DISCUSSION

We grew *Chlamydomonas reinhardtii* in chemostats to explore the phenotypic plasticity of elemental and macromolecular pools in response to growth rate and resource limitation.

Cell morphology

Changes in growth rate resulted in large changes in cell morphology. Under fast growth (80% μ_{max}), cell dry weight (a proxy for cell size) was significantly smaller (Pairwise comparison Tukey's HSD $p < 0.05$) than at slow growth (20% of μ_{max}), regardless of environmental resource limitation (Figure 1; File S2 in the Supporting Information: Figure S2.1 and Table S2). For most treatments under slow growth, cell length was ~10 µm. The one exception was the low light treatment, in which cell sizes were more than threefold smaller and converged on those observed in the fast growth treatments (~7.5 µm length). Cell volume and width showed the same pattern (File S2: Figure S2.2). Similar observations have been made in green algae previously (Schlesinger et al., 1981). Under saturating light conditions (which was the case in all our treatments except the low light), an inverse relationship between cell size and growth rate was observed. Similar to our findings, the study of Schlesinger et al. (1981) also noted that with

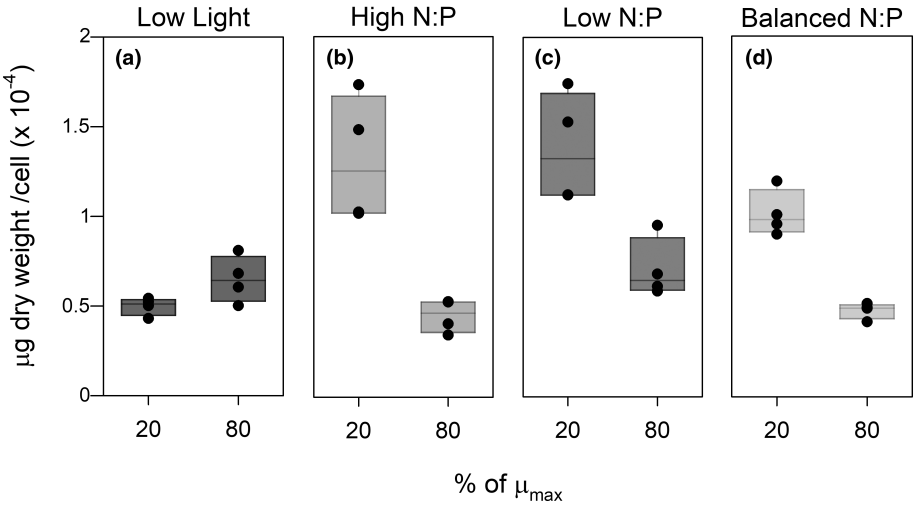

FIGURE 1 Relationship between dry weight per cell and growth rate, showing that cell size decrease depends on resource limitation and growth rate. (a) 60 µmol·m^{-2}·s^{-1}, (b) 80:1 N:P ratio, (c) 6:1 N:P ratio, and (d) 16:1 N:P ratio.

decreasing light intensity, the relationship between cell size and growth rate weakened. Variation in size affects numerous cell processes, including physiological rates and efficiency of resource acquisition. For example, in unicellular algae, variability in cell size has been shown to influence rates of metabolism (growth, photosynthesis, and respiration), light absorption (Finkel, 2001; Raven, 1984), nutrient uptake, and cell nutrient quotas (Hein et al., 1995; Pasciak & Gavis, 1974). In spherical cells, decreases in size have been shown to increase the surface area to volume ratio, facilitating nutrient uptake and nutrient diffusion (Raven, 1984). Hence, in our experiments, the reduction in cell volume at faster growth likely reflected morphological acclimation by *Chlamydomonas reinhardtii* to maximize surface area to volume ratios in order to acquire limiting nutrients. Small cells are more efficient in light harvesting (Raven, 1984), which might explain why we observed consistently small cells in the low light treatment. On the other hand, larger cells may be able to store more nutrients intracellularly, an acclimation that is potentially advantageous when growth conditions change (Finkel et al., 2010; Mei et al., 2009). This, however, is not consistent with our data, as large cells showed lower N and P contents (% dry weight). As cell size is highly species dependent, the size to which cells converge under slow growth might be the smallest developmentally feasible size for a given genotype and thus might be a useful metric for trait-based approaches.

Macromolecular composition

Biomass composition can be described in terms of macromolecules, the major biochemical constituents that make up biomass. Here, we measured carbohydrate, lipid, protein, RNA, DNA, chlorophyll, and ATP and could explain 61%–108% of total dry weight (Figure 2, File S3 in the Supporting Information: Figure S3.1). In general, a larger fraction of the cell dry weight could be accounted for in the measured macromolecular pools under slow growth relative to fast growth. Carbohydrates, lipids, and protein were the most dominant macromolecular pools measured across all growth rates and resource limitations (Figure 2). This is in line with other studies on microalgae (Finkel et al., 2016).

Chlamydomonas reinhardtii is known for its high lipid and carbohydrate content, which is why it is well-suited for biotechnological applications (Burlacot et al., 2019; Morales-Sánchez et al., 2020; Scaife et al., 2015). The observed range of macromolecules depended on both the type of limiting resource (light or nutrients) and growth rate, as well the interaction among resources and growth rate ($p < 0.05$, for details on individual macromolecules, please see File S1: Table S1.1). The macromolecular pool composition of cells grown under low light conditions was considerably different from other treatments, regardless of growth rate but especially for slow-growing cells. For example, cells grown in the low light treatment had elevated proportions of chlorophyll, ATP, lipids, and RNA but lower carbohydrate, compared to other resource limitations (Figure 2) as discussed below. Despite our efforts to provide a complete overview of the macromolecular constituents of *C. reinhardtii*, there were instances where less than 100% of the dry weight could be accounted for (Figure 2). We suspect unquantified cellular pools such as polyphosphates and biominerals (e.g., calcium and silica, measured as ash) could account for these discrepancies. Although elemental and macromolecular variability

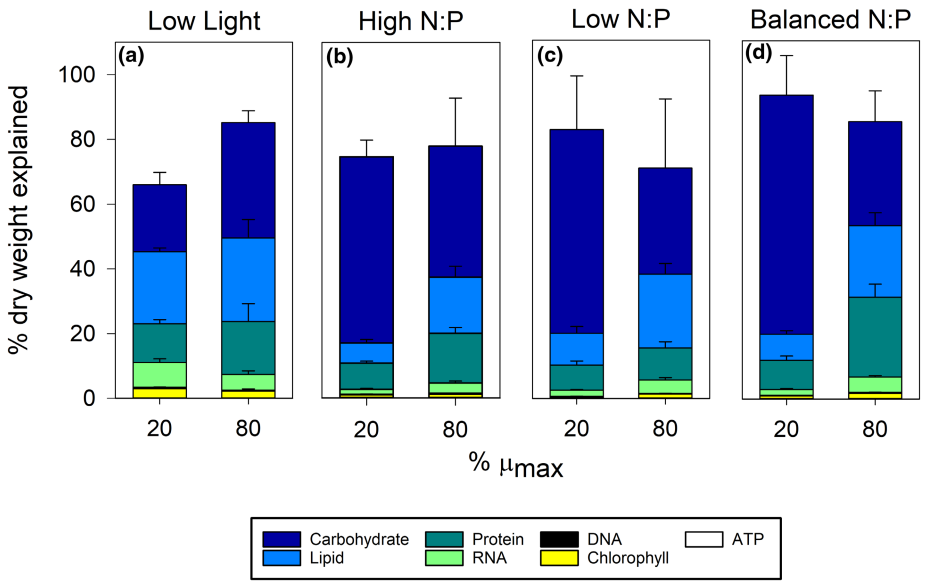

FIGURE 2 Percentage of dry weight that can be explained by macromolecular pools. Error bars show standard deviation.

among taxa is well documented (Finkel et al., 2010, 2016), our observations illustrate the flexibility within a single strain with implications for future efforts that aim to explain elemental and macromolecular dynamics in aquatic systems.

Elemental composition and molecules

Like all living things, *Chlamydomonas reinhardtii* requires a variety of essential elements to carry out cellular functions. To a large degree, the C, N, and P contents of *C. reinhardtii* reflected its macromolecular composition. Here, to assess variation in elemental composition, we measured biomass pools of C, N, and P, then normalized these elemental pools to both dry weight (Figure 3a–c) and cell abundance (File S3: Figure S3.2). We also calculated the contribution of each macromolecule to each of the three elements (Figure 4, File S4 in the Supporting Information: Figure S4; e.g., carbon bound in lipids), based on Sterner and Elser (2002). Overall, the macromolecular pools explained 70%–90%, 34%–81%, and 46%–117% of the measured biomass C, N, and P, respectively (Figure 4). Carbohydrates, lipids, and protein themselves accounted for most (62%–84%) of the measured biomass C (Figure 4a–d). Contributions of these macromolecular pools varied with resource limitation, growth, and the interactions between these factors (File S4: Table S4).

Carbon and C-rich molecules

Carbon is a fundamental component of all organic molecules. Previous studies have found that cellular C content (% dry mass contributed by C) of organismal biomass is up to 10-fold less variable than P (Andersen & Hessen, 1991; Elser et al., 1996; Sterner & Elser, 2002). Consistent with this, cellular C contents (% dry weight) were relatively stable across resource ($F = 2.11$, $p = 0.125$) and growth rate ($F = 1.24$, $p = 0.276$), ranging between 44% and 53% (Figure 3a), considerably less variable than N and P contents. As expected, the major macromolecules constituting total C in *Chlamydomonas reinhardtii* were carbohydrates and lipids (Figure 4a–d).

Lipids are important components of cellular membranes and are precursors for signaling molecules (Arts et al., 2009). Together with carbohydrates such as starch and sugars, these two macromolecular pools can serve as energy reserves. Except for in the low light treatment, variation in the contribution of carbohydrates explained a large fraction (47%–52%) of the variability across treatments in biomass C (Carbohydrate-C) at slow-growth rates (Figure 4a–d). In the low light

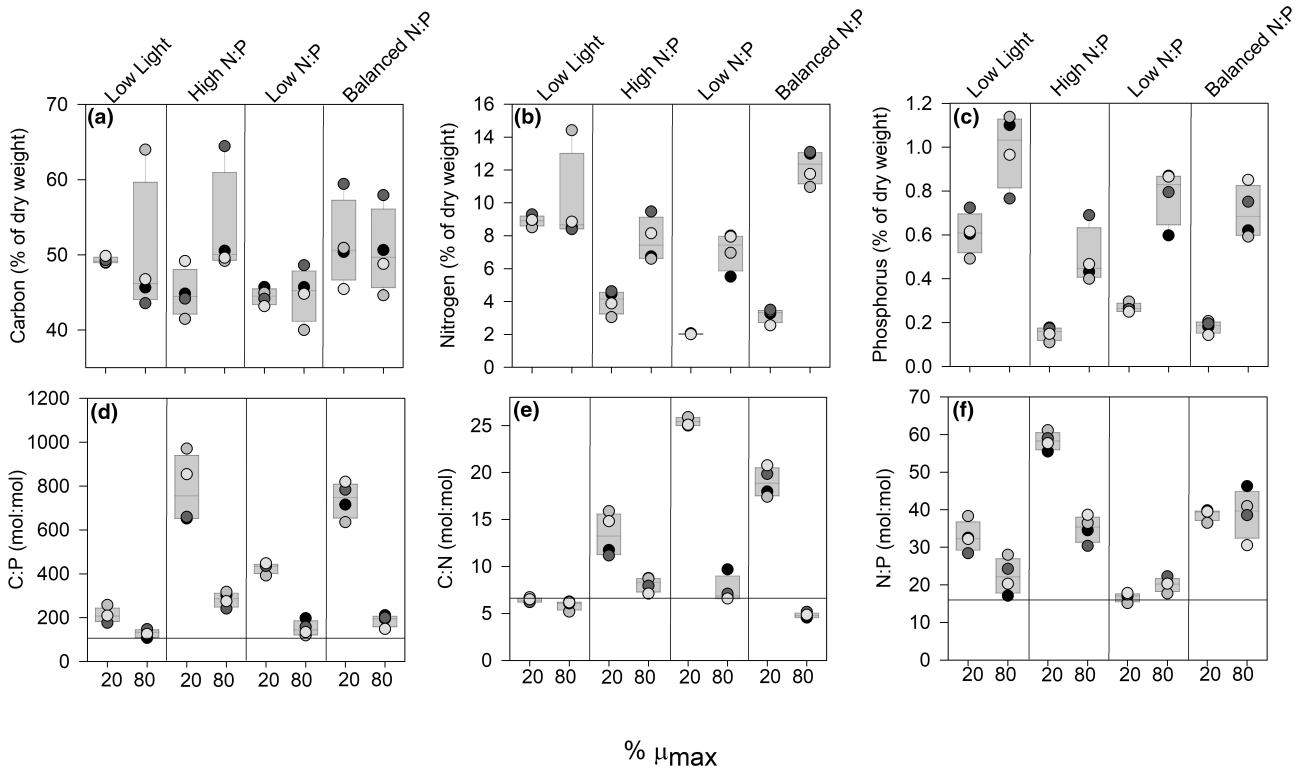

FIGURE 3 Elemental pools of carbon (a), nitrogen (b) and phosphorus (c) normalized to dry weight in *Chlamydomonas reinhardtii* in response to growth rate and resource limitation. Molar ratios of these key elements to each other are depicted in (d–f). The horizontal line in (d–f) shows the Redfield ratio for orientation.

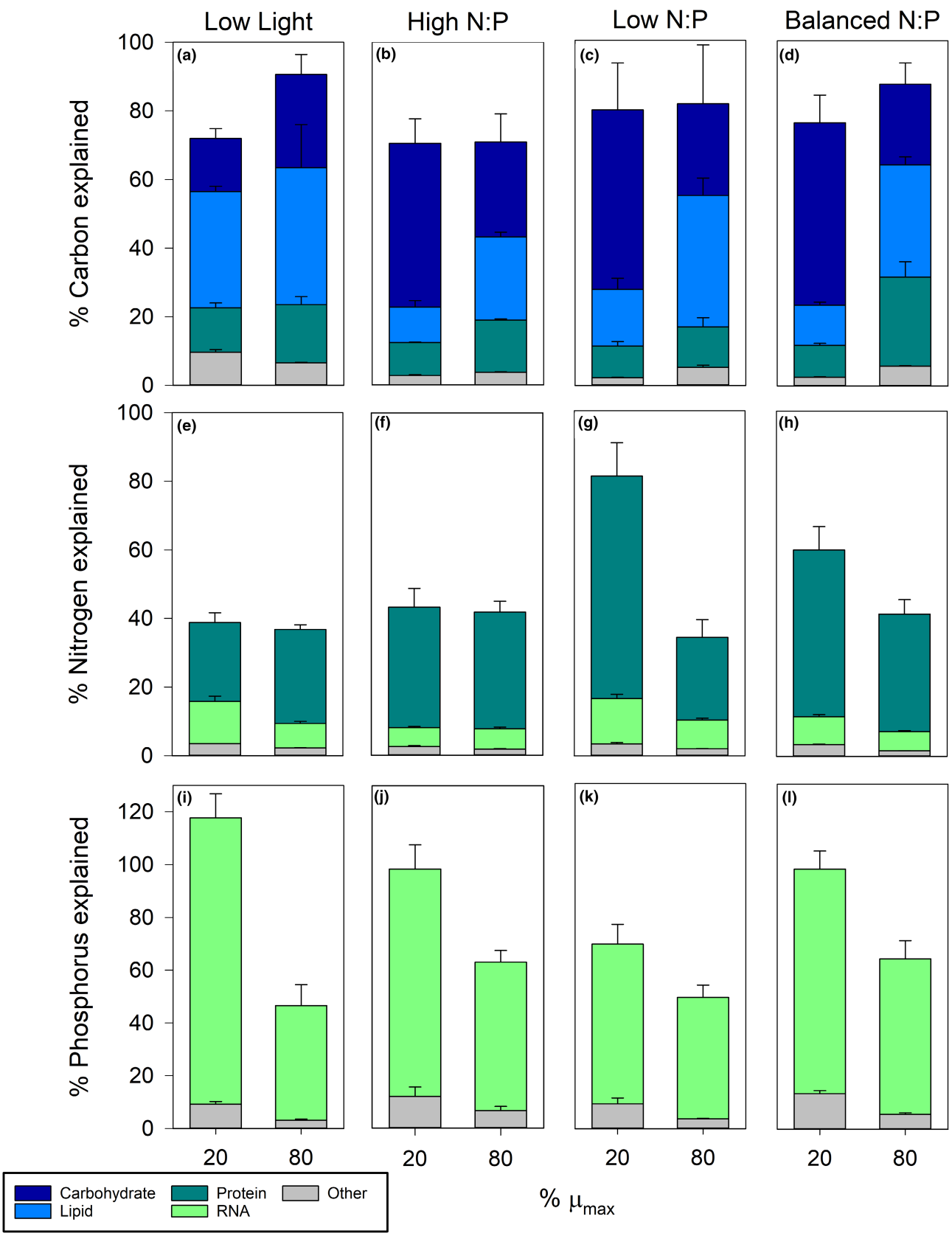

FIGURE 4 Percentage of elements carbon (a–d), nitrogen (e–h), and phosphorus (i–l) explained by different macromolecular pools. Macromolecules are depicted only when the respective elements explained at least 15% of the total elemental pool measured. Macromolecules such as RNA, DNA, chlorophyll, and ATP are summed up, depending on treatment, as others (gray). See File S4 for additional information. Error bars show standard deviation.

treatment, lipids explained most of the biomass C (Lipid-C), and generally, across all treatments explained 10%–39%. At slow growth, there was significantly more lipid-C and less carbohydrate-C contributing to total C than in any of the other treatments (Pairwise comparison Tukey's HSD, $p < 0.001$). These differences partially disappeared at fast growth (Figure 4a–d).

The differential allocation of C into carbohydrates versus lipids that we observed here under low light conditions had previously been documented mainly under environmental stress. An increase in lipid content could often be seen in N-depleted environments (Dean et al., 2010; James et al., 2011). In our experiments, the highest lipid and lowest carbohydrate contents were observed in slow-growing cells under low light (Figure 2a). However, in fast-growing cells, cellular lipid pools increased, and carbohydrate pools decreased in all other resource limitations and reached similar proportions to those found under low light conditions. While biomass C content did not differ, our results imply a shift between storing C (energy) in carbohydrates versus lipids, depending on growth rate and resource limitation. This trade-off may be due to differences in the energetics of lipid versus carbohydrate synthesis and use. In *Chlamydomonas reinhardtii* alterations in energy management pathways have been found to influence biomass content and composition (Burlacot et al., 2019). This might reflect the energetic investment required for lipid synthesis relative to carbohydrates, with lipid synthesis being more energetically costly (Johnson & Alric, 2013). Although lipids return more cellular energy (in the form of ATP) per C atom than carbohydrates when oxidized, the *net* energy return (inclusive of energy invested in synthesis) is lower (Johnson & Alric, 2013). When *C. reinhardtii* is grown photoautotrophically (i.e., with light as an energy source and CO_2 as the sole C source), carbohydrate synthesis appears an efficient way to store C (Johnson & Alric, 2013). In contrast, the synthesis of fatty acids, a precursor intermediate to lipids, represents a significant loss of C, as one third of the fixed C is lost during synthesis (Johnson & Alric, 2013). Hence, while carbohydrates represent a better form of C storage than lipids, the energy return upon lipid oxidation (~6.7 ATP equivalents per carbon atom) is greater than for carbohydrate oxidation (~5.3 ATP equivalents per C; Johnson & Alric, 2013). Synthesizing lipids rather than carbohydrates therefore appears to be a useful strategy when C is not limiting but energy is, for example, in our low light treatments.

Protein was also a large contributor to cellular C pools and accounted for a larger fraction of biomass C at fast growth than under slow growth. The highest contribution of protein to biomass C pools was observed in the balanced N:P treatment at fast growth (26%). At slow growth, the contribution of protein to biomass C was less variable among the different resource limitations. That we observed the highest contribution of protein to C (Protein-C) was perhaps not unexpected, since faster growth likely requires higher concentrations of ribosomal proteins and enzymes (Sterner & Elser, 2002). In other algae, protein has been observed to be the largest contributor to cellular C, ranging from 31% to 43% (Ebenezer et al., 2022; Finkel et al., 2016). This demonstrates the high variability of protein content across different algal species. Other macromolecules, such as RNA, chlorophyll *a*, DNA, and ATP only contributed <10% of the biomass C (File S4: Figure S4a–c), regardless of the growth rate or resource limitation, in line with other studies (Ebenezer et al., 2022, Finkel et al., 2016).

Nitrogen and N-rich macromolecules

Nitrogen is a crucial constituent of proteins and is also required to produce nucleic acids and chlorophyll. *Chlamydomonas reinhardtii* can assimilate N from various sources, including amino acids, nitrate, ammonium, and urea, depending on the availability in the environment (Bellido-Pedraza et al., 2020; Harris et al., 2009). Here, we provided N only as nitrate. Cellular growth based on nitrate versus other forms of N has been shown to critically influence different aspects of photophysiology (Gérin et al., 2016). In contrast to cellular C, cellular N content was more responsive to changes in growth rate and resource availability, with %N and varying up to 4.5-fold (Figure 3b). The percentage of N shifted significantly in response to growth rate ($F = 106$, $p < 0.001$), resource limitation ($F = 21.7$, $p < 0.001$), and their interaction ($F = 12.8$, $p < 0.001$). A notable exception was found in the low light treatment, in which %N was highest and did not change with growth rate (Pairwise comparison Tukey's HSD, $p = 0.232$).

Nitrogen is an important component of light-harvesting pigments; chlorophyll, for example, contains 6.5% N by mass (Sterner & Elser, 2002). The major pigments of green algae are chlorophyll *a* and *b* (Nozaki, 2015). Here, under low light conditions, all available dissolved N was likely taken up, since production of light-harvesting pigments is typically mobilized under low light conditions (Lewitus & Caron, 1990). In line with that, we observed the highest chlorophyll *a* content in the low light treatment at both growth rates (Figure 2 and File S4: Figure S4). Unfortunately, we did not quantify chlorophyll *b*. However, the most nitrogen-rich macromolecule typically is protein (Sterner & Elser, 2002). In our study, we quantified several N-containing macromolecular pools, including protein, chlorophyll, RNA, DNA, and ATP (Figure 4e–h, File S4: Figure S4e–h). Indeed, protein (22%–64%), was the macromolecule that explained most of biomass N in *Chlamydomonas reinhardtii*, followed by RNA (5%–13%; Figure 4e–h). Protein contributions varied with resource ($F = 19.4$, $p < 0.001$), growth rate ($F = 45.5$, $p < 0.001$), and

their interaction ($F = 27.5$, $p < 0.001$). We expected faster growing cells to have higher cellular N content due to the increased need for enzymes to support rapid growth (Brown, 1991; Sterner & Elser, 2002). Consistent with this, biomass N contents generally increased at faster growth (Figure 3b), but the fraction of N that we could attribute to nitrogenous macromolecules, including protein, was similar (Figure 4e,f) or even lower (Figure 4g,h) at fast growth (accounting for ~40% of biomass N). There were no statistical differences in the estimated contributions of protein to biomass N pools across all treatments at fast growth (Pairwise comparison Tukey's HSD, $p > 0.05$). Hence, we are not able to explain why and how biomass N content increased with fast growth. We suspect that, under rapid growth, *C. reinhardtii* accumulates significant amounts of N in forms or pools that we did not measure, such as inorganic N. Indeed, considerable intracellular storage of inorganic N at fast growth has been observed previously (Collos & Berges, 2003; Cunningham & Maas, 1978). It has previously been suggested that fast-growing cells are not as severely limited by nutrient supply as slow-growing cells (Boer et al., 2010). Our data confirm this expectation, as slow-growing cells appear more susceptible to nutrient limitation than rapidly growing cells, potentially enabling intracellular accumulation of N at fast growth rates. However, there are also studies demonstrating that, at slow growth rates, excess uptake (also known as luxury uptake) of the non-limiting nutrients can lead to cellular N:P ratios that match the supply N:P ratios (Rhee, 1978) while at higher growth rates, the cellular N:P converges (Elrifi & Turpin, 1985; Goldman et al., 1979), eventually reaching an "optimal" N:P under exponential growth (Hillebrand et al., 2013; Klausmeier et al., 2004). Whether or not *C. reinhardtii* relies more on luxury N at fast or at slow growth needs further investigation, including studies quantifying intracellular inorganic and organic N pools.

Phosphorus and P-rich macromolecules

Phosphorus is an essential element for energy and electron transfer (in ATP and NADPH), for construction of nucleic acids, and for membrane structure. *Chlamydomonas reinhardtii* generally obtains P as phosphate (PO_4^{3-}) present in the environment (Harris et al., 2009). In contrast to cellular C but similar to cellular N, cellular P contents (Figure 3c) were highly responsive to changes in growth rate ($F = 142$, $p < 0.001$) and resource availability ($F = 30$, $p < 0.001$), with %P varying up to 6.5-fold. We measured the P-containing macromolecules RNA, DNA, and ATP, and although these pools were estimated to explain the majority of biomass P at slow growth (ranging 69%–117%), these macromolecular pools only explained 46%–64% of the measured biomass P pools at fast growth (Figure 4i–l). Cellular pools of RNA accounted for the majority (43%–58%) of biomass P (RNA-P), with this contribution varying with resource limitation ($F = 18.5$, $p < 0.001$), growth ($F = 202.4$, $p < 0.001$), and their interaction ($F = 21$, $p < 0.001$; File S1: Table S1.3). The question therefore arises about which cellular P pools other than RNA account for increased P content under fast growth. Phosphorus bound in DNA and ATP together explained less than 6% of total organismal P under fast growth (File S4: Figure S4i–l). One possibility is phospholipids, in which phosphate is esterified to the *sn*-3 position of the glycerol backbone (Arts et al., 2009). We did not directly quantify phospholipids, but our measurements of total lipids can be used to constrain the P contained in phospholipids. Assuming that phospholipids make up ~2% of dry weight (Taipale et al., 2015), this would suggest that between 8% and 11% of the total lipids that we measured under fast growth would be in the form of phospholipids. Phospholipids contain 4.2% P (Sterner & Elser, 2002). Hence, we estimate that biomass P potentially attributable to phospholipids under fast growth conditions varied between ~13% (low light), ~16% (low N:P), ~25% (balanced N:P), and ~48% (high N:P). Similar contributions of phospholipids in explaining total organismal P have been found previously in marine phytoplankton (20%–60%, Ebenezer et al., 2022). Microalgae are also capable of luxury P uptake, resulting in intracellular accumulation of P pools. The bulk of P acquired during luxury uptake appears to be stored as polyphosphates (Solovchenko et al., 2019). Hence, the additional "missing" P in our experiments might have been present in polyphosphates. Polyphosphates are ubiquitous in microalgal cells, carrying out multiple functions (Solovchenko et al., 2019; Zhu et al., 2015), and are known P reserves in *C. reinhardtii* (Plouviez et al., 2022; Werner et al., 2007). After lipids, polyphosphates have been found to be the second largest P pool in marine phytoplankton, contributing ~20% of cellular P (Ebenezer et al., 2022).

In *Chlamydomonas reinhardtii*, the supply of dissolved P in the media has been documented to influence luxury uptake of P, while light supply does not (Plouviez et al., 2023). Our data however suggest an association between luxury P accumulation and growth rate, rather than dissolved P or light supply. This relationship should be investigated further. Regardless, here it appears that there is a substantial allocation of P either to lipids or polyphosphates (together potentially ~35%–70% of total organismal P) that is growth rate dependent. These pools could account for as much biomass P as RNA (~40%–60% of biomass P).

In summary, measurements of macromolecular pools revealed that carbohydrates, lipids, protein, and nucleic acids explained between 60% and 80% of the measured cell dry weight, with particularly large variations observed in carbohydrates, lipids, and proteins depending on resource limitation and growth rate. Variations in carbohydrate and lipid appeared to underlie changes in cell

cellular C, with carbohydrates often accounting for upward of 60% of the cellular C quotas in slow-growth treatments. Intriguingly, measured cell protein and nucleic acids generally accounted for <50% of the cell N quota, suggesting an unquantified source of cellular N. Cellular P quotas were dominated by P in RNA, and RNA content generally varied with growth rate. However, although the proportion of RNA in cell dry mass did generally increase with growth rate, RNA often accounted for a greater fraction of cellular P pools under conditions of slow growth, contrary to expectations. This indicates that fast-growing cells disproportionately accumulated P into an unquantified cellular pool.

Elemental stoichiometry

Here, to assess variation in elemental stoichiometry of *Chlamydomonas reinhardtii* cells, we calculated the molar ratios of C, N, and P (Figure 3d–f). As described above, the relatively invariant cellular C contents, together with more variable N and P contents, resulted in large variations in cellular elemental ratios (Figure 3d–f). At slow-growth rates, C:P ratios varied from 175 to 971, C:N ratios from 4.5 to 25, and N:P ratios from near Redfield (15.1) up to 61.2 (Figure 3d–f). Both C:P and C:N ratios tended to be elevated at slow growth relative to rapid growth (Figure 3d–f), with the stoichiometry of faster growing cells often approaching the Redfield ratio (Figure 3d–f). Eukaryotic phytoplankton are known to exhibit considerable stoichiometric plasticity, with nutrient availability being important drivers of C:P and C:N ratios (Tanioka & Matsumoto, 2020). Here, we show that both growth rate and resource limitation, as well as their interaction, drive *C. reinhardtii* C:N:P stoichiometry (all $p < 0.001$, for F values please see File S1: Table S1.2). Notably, elemental stoichiometry was relatively constant for cells grown under low light conditions (regardless of growth rate; Figure 3d–f). To the best of our knowledge, this has not been explicitly studied in *C. reinhardtii*, but other studies have reported different effects of low or limiting light conditions on elemental ratios (Finkel et al., 2010; Hessen et al., 2002; Leonardos & Geider, 2004). For example, in line with our findings, the green algae *Selenastrum capricornutum*, has been reported to increase elemental ratios (C:P and C:N) from low light conditions to the same light intensity we used here (200 μmol photons · m^{-2} · s^{-1}; Hessen et al., 2002).

Implications for the growth rate hypothesis

A key component of the theory of ecological stoichiometry is the growth rate hypothesis (GRH; Elser et al., 2000, Sterner & Elser, 2002). The GRH states that variation in organismal stoichiometry (in particular, C:P and N:P ratios) is driven by growth-dependent allocation to P-rich ribosomal RNA that leads to disproportionate increases in biomass P content (relative to N content). The GRH was originally formulated to help explain observed differences in C:N:P ratios of different species of zooplankton (Andersen & Hessen, 1991; Elser et al., 1996; Sterner et al., 1992) and has since been applied across a wide range of organisms (Hessen et al., 2013; Isanta-Navarro et al., 2022). Specifically, the GRH proposes first that, under rapid growth, biomass P content (percentage of dry mass) increases disproportionately relative to C and N contents, and thus C:P and N:P ratios are lower under rapid growth. Second, the GRH proposes that this increase in P content reflects a disproportionate increase (relative to other macromolecular pools) in allocation to P-rich RNA. Thus, under the GRH, it is also expected that RNA-P (the percentage of organismal P that can be explained by P in RNA) increases with faster growth, as has been shown in some cases (Elser et al., 2003). However, our data show that in *Chlamydomonas reinhardtii*, the different components of the GRH differed in their robustness. The most reliable component was the first, that %P of organismal biomass increases with faster growth, which was true under all resource manipulations that we tested here (Figure 3c). We found %C to be least variable across all treatments and thus conclude that %P was driving changes in C:P. However, we also found that %N typically increased with growth rate. As a result, the decrease in biomass N:P ratios predicted by the GRH was only observed under the low light and high N:P treatments. RNA content increased with faster growth under all resource limitations but not the low light treatment. Hence, our observations (Figure 2a–d) are largely consistent with the predictions of the second component of the GRH. However, contrary to expectations that follow from the GRH, the contribution of RNA to biomass P pools did not increase in any of the resource manipulations. Instead, the fraction of P content explained by the contribution of P contributed by RNA decreased with faster growth in all treatments (Figure 4i–l). Taken together, these observations indicate that with faster growth, *C. reinhardtii* accumulates P in an intracellular pool we did not measure. Moreover, this pool appears to increase with growth rate even more than cellular RNA pools. We suspect this may reflect accumulation of a storage molecule, such as polyphosphate, during periods of rapid growth. We conclude that the utility of the GRH and its proposed mechanisms are context-dependent in photoautotrophic *C. reinhardtii*. Specifically, our results indicate that the GRH is most robust under high N:P and performs worst under low light conditions, helping to clarify the domain of conditions under which the GRH holds or fails to hold, an important goal identified by previous authors (Hessen et al., 2013, Isanta-Navarro et al., 2022).

CONCLUSIONS

To summarize, we observed that this genotype of *Chlamydomonas* harbors considerable ability to dynamically adjust levels and composition of elemental and macromolecular pools in its biomass. Elemental contents in *C. reinhardtii* varied depending on the growth rate but were also influenced by growth conditions such as chemical and physical parameters of the growth environment. Low light conditions led to the largest changes in cellular macromolecular composition. This might be of particular note in understanding the potential range of biochemical and stoichiometric composition of algae growing during low light conditions, such as those found at depth or in turbid waters where light is absorbed quickly. Understanding the elemental and macromolecular plasticity of *C. reinhardtii* and other photoautotrophs will be important for elucidating how physiological adjustments in response to changing environmental conditions influence resource use and ultimately impact higher trophic levels and biogeochemical cycling.

AUTHOR CONTRIBUTIONS

James J. Elser: Conceptualization (equal); funding acquisition (lead); project administration (lead); writing – original draft (supporting); writing – review and editing (supporting). **Matthew J. Church:** Conceptualization (equal); funding acquisition (supporting); project administration (supporting); writing – original draft (supporting); writing – review and editing (supporting). **Logan M. Peoples:** Conceptualization (equal); investigation (supporting); methodology (supporting). **Benedicta Bras:** Investigation (supporting); methodology (supporting). **Jana Isanta-Navarro:** Conceptualization (equal); data curation (lead); formal analysis (lead); investigation (lead); methodology (lead); visualization (lead); writing – original draft (lead); writing – review and editing (lead).

ACKNOWLEDGMENTS

We are grateful to Frank Rosenzweig for support with chemostat design and theory, as well as his comments on this article. We cordially thank Adam Baumann and Sydni Racki for analytical support. Meghan Heffernan, Rustin Bielski, and Vivian Klotz are acknowledged for support in culture maintenance and experimental assistance. We also thank all members of the Rules of Life team for inspiring discussions and support. This work was supported by the US National Science Foundation Rules of Life program (DEB-1930816 to JJE and MJC).

ORCID

Jana Isanta-Navarro https://orcid.org/0000-0002-6168-4499
Logan M. Peoples https://orcid.org/0000-0002-0163-2769
Matthew J. Church https://orcid.org/0000-0002-6166-8579
James J. Elser https://orcid.org/0000-0002-1460-2155

REFERENCES

Andersen, T., & Hessen, D. O. (1991). Carbon, nitrogen, and phosphorus content of freshwater zooplankton. *Limnology and Oceanography*, *36*, 807–814.
Arts, M. T., Brett, M. T., & Kainz, M. (2009). *Lipids in aquatic ecosystems*. Springer Science & Business Media.
Bellido-Pedraza, C. M., Calatrava, V., Sanz-Luque, E., Tejada-Jiménez, M., Llamas, Á., Plouviez, M., Guieysse, B., Fernández, E., & Galván, A. (2020). *Chlamydomonas reinhardtii*, an algal model in the nitrogen cycle. *Plants*, *9*, 903.
Boer, V. M., Crutchfield, C. A., Bradley, P. H., Botstein, D., & Rabinowitz, J. D. (2010). Growth-limiting intracellular metabolites in yeast growing under diverse nutrient limitations. *MBoC*, *21*, 198–211.
Brown, G. C. (1991). Total cell protein concentration as an evolutionary constraint on the metabolic control distribution in cells. *Journal of Theoretical Biology*, *153*, 195–203.
Burlacot, A., Peltier, G., & Li-Beisson, Y. (2019). Subcellular energetics and carbon storage in *Chlamydomonas*. *Cell*, *8*, 1154.
Caron, D. A., Goldman, J. C., Andersen, O. K., & Dennett, M. R. (1985). Nutrient cycling in a microflagellate food chain: II. Population dynamics and carbon cycling. *Marine Ecology Progress Series*, *24*, 243–254.
Collos, Y., & Berges, J. (2003). Marine ecology. In *Nitrogen metabolism in phytoplankton* (pp. 262–280). EOLSS.
Cunningham, A., & Maas, P. (1978). Time lag and nutrient storage effects in the transient growth response of *Chlamydomonas reinhardii* in nitrogen-limited batch and continuous culture. *Journal of General Microbiology*, *104*, 227–231.
De Jong, G. (2005). Evolution of phenotypic plasticity: Patterns of plasticity and the emergence of ecotypes. *New Phytologist*, *166*, 101–118.
Dean, A. P., Sigee, D. C., Estrada, B., & Pittman, J. K. (2010). Using FTIR spectroscopy for rapid determination of lipid accumulation in response to nitrogen limitation in freshwater microalgae. *Bioresource Technology*, *101*, 4499–4507.
Dudgeon, D. (2019). Multiple threats imperil freshwater biodiversity in the Anthropocene. *Current Biology*, *29*, R960–R967.
Ebenezer, V., Hu, Y., Carnicer, O., Irwin, A. J., Follows, M. J., & Finkel, Z. V. (2022). Elemental and macromolecular composition of the marine Chloropicophyceae, a major group of oceanic photosynthetic picoeukaryotes. *Limnology and Oceanography*, *67*, 540–551.
Elrifi, I. R., & Turpin, D. H. (1985). Steady-state luxury consumption and the concept of optimum nutrient ratios: A study with phosphate and nitrate limited *Selenastrum minutum* (chlorophyta). *Journal of Phycology*, *21*, 592–602.
Elser, J. J., Acharya, K., Kyle, M., Cotner, J., Makino, W., Markow, T., Watts, T., Hobbie, S., Fagan, W., Schade, J., Hood, J., & Sterner, R. W. (2003). Growth rate-stoichiometry couplings in diverse biota. *Ecology Letters*, *6*, 936–943.
Elser, J. J., Dobberfuhl, D. R., MacKay, N. A., & Schampel, J. H. (1996). Organism size, life history, and N:P stoichiometry: Toward a unified view of cellular and ecosystem processes. *Bioscience*, *46*, 674–684.
Elser, J. J., Marzolf, E. R., & Goldman, C. R. (1990). Phosphorus and nitrogen limitation of phytoplankton growth in the freshwaters of North America: A review and critique of experimental enrichments. *Canadian Journal of Fisheries and Aquatic Sciences*, *47*, 1468–1477.
Elser, J. J., Sterner, R. W., Gorokhova, E., Fagan, W. F., Markow, T. A., Cotner, J. B., Harrison, J. F., Hobbie, S. E., Odell, G. M., &

Weider, L. W. (2000). Biological stoichiometry from genes to ecosystems. *Ecology Letters*, *3*, 540–550.

Finkel, Z. V. (2001). Light absorption and size scaling of light-limited metabolism in marine diatoms. *Limnology and Oceanography*, *46*, 86–94.

Finkel, Z. V., Beardall, J., Flynn, K. J., Quigg, A., Rees, T. A. V., & Raven, J. A. (2010). Phytoplankton in a changing world: Cell size and elemental stoichiometry. *Journal of Plankton Research*, *32*, 119–137.

Finkel, Z. V., Follows, M. J., Liefer, J. D., Brown, C. M., Benner, I., & Irwin, A. J. (2016). Phylogenetic diversity in the macromolecular composition of microalgae. *PLoS ONE*, *11*, e0155977.

Fusco, G., & Minelli, A. (2010). Phenotypic plasticity in development and evolution: Facts and concepts. *Philosophical Transactions of the Royal Society B*, *365*, 547–556.

Gardner, W. S., Frez, W. A., Cichocki, E. A., & Parrish, C. C. (1985). Micromethod for lipids in aquatic invertebrates. *Limnology and Oceanography*, *30*, 1099–1105.

Garland, T., & Kelly, S. A. (2006). Phenotypic plasticity and experimental evolution. *Journal of Experimental Biology*, *209*, 2344–2361.

Geider, R., & La Roche, J. (2002). Redfield revisited: Variability of C:N:P in marine microalgae and its biochemical basis. *European Journal of Phycology*, *37*, 1–17.

Gérin, S., Leprince, P., Sluse, F. E., Franck, F., & Mathy, G. (2016). New features on the environmental regulation of metabolism revealed by modeling the cellular proteomic adaptations induced by light, carbon, and inorganic nitrogen in *Chlamydomonas reinhardtii*. *Frontiers in Plant Science*, *7*, 1158.

Goldman, J. C., McCarthy, J. J., & Peavey, D. G. (1979). Growth rate influence on the chemical composition of phytoplankton in oceanic waters. *Nature*, *279*, 1–215.

Gorokhova, E., & Kyle, M. (2002). Analysis of nucleic acids in *Daphnia*: Development of methods and ontogenetic variations in RNA-DNA content. *Journal of Plankton Research*, *24*, 511–522.

Harris, E. H., Stern, D. B., & Witman, G. (2009). *The Chlamydomonas sourcebook* (2nd ed.). Elsevier/Academic Press.

Hein, M., Pedersen, M., & Sand-Jensen, K. (1995). Size-dependent nitrogen uptake in micro- and macroalgae. *Marine Ecology Progress Series*, *118*, 247–253.

Hessen, D. O., Elser, J. J., Sterner, R. W., & Urabe, J. (2013). Ecological stoichiometry: An elementary approach using basic principles. *Limnology and Oceanography*, *58*, 2219–2236.

Hessen, D. O., Færøvig, P. J., & Andersen, T. (2002). Light, nutrients, and P:C ratios in algae: Grazer performance related to food quality and quantity. *Ecology*, *83*, 1886–1898.

Hessen, D. O., Hafslund, O. T., Andersen, T., Broch, C., Shala, N. K., & Wojewodzic, M. W. (2017). Changes in stoichiometry, cellular RNA, and alkaline phosphatase activity of *Chlamydomonas* in response to temperature and nutrients. *Frontiers in Microbiology.*, *8*, 18.

Hillebrand, H., Steinert, G., Boersma, M., Malzahn, A., Meunier, C. L., Plum, C., & Ptacnik, R. (2013). Goldman revisited: Faster-growing phytoplankton has lower N : P and lower stoichiometric flexibility. *Limnology and Oceanography*, *58*, 2076–2088.

Holm-Hansen, O. (1973). The use of ATP determinations in ecological studies. *Bulletins from the Ecological Research Committee*, *17*, 215–222.

Holm-Hansen, O., Lorenzen, C. J., Holmes, R. W., & Strickland, J. D. H. (1965). Fluorometric determination of chlorophyll. *ICES Journal of Marine Science*, *30*, 3–15.

Huisman, J., Matthijs, H. C. P., Visser, P. M., Balke, H., Sigon, C. A. M., Passarge, J., Weissing, F. J., & Mur, L. R. (2002). Principles of the light-limited chemostat: Theory and ecological applications. *Antonie Van Leeuwenhoek*, *81*, 117–133.

Isanta-Navarro, J., Prater, C., Peoples, L. M., Loladze, I., Phan, T., Jeyasingh, P. D., Church, M. J., Kuang, Y., & Elser, J. J. (2022). Revisiting the growth rate hypothesis: Towards a holistic stoichiometric understanding of growth. *Ecology Letters*, *25*, 2324–2339.

James, G. O., Hocart, C. H., Hillier, W., Chen, H., Kordbacheh, F., Price, G. D., & Djordjevic, M. A. (2011). Fatty acid profiling of *Chlamydomonas reinhardtii* under nitrogen deprivation. *Bioresource Technology*, *102*, 3343–3351.

Johnson, X., & Alric, J. (2013). Central carbon metabolism and electron transport in *Chlamydomonas reinhardtii*: Metabolic constraints for carbon partitioning between oil and starch. *Eukaryotic Cell*, *12*, 776–793.

Karl, D. M., Dore, J. E., Hebel, D. V., & Winn, C. (1991). Procedures for particulate carbon, nitrogen, phosphorus and total mass analyses used in the us-JGOFS Hawaii Ocean time-series program. In D. C. Hurd & D. W. Spencer (Eds.), *Geophysical monograph series* (pp. 71–77). American Geophysical Union.

Kilham, S. S., Kreeger, D. A., Lynn, S. G., Goulden, C. E., & Herrera, L. (1998). COMBO: A defined freshwater culture medium for algae and zooplankton. *Hydrobiologia*, *377*, 147–159.

Klausmeier, C. A., Litchman, E., & Levin, S. A. (2004). Phytoplankton growth and stoichiometry under multiple nutrient limitations. *Limnology and Oceanography*, *49*, 1463–1470.

Kyle, M., Watts, T., Schade, J., & Elser, J. J. (2003). A microfluorometric method for quantifying RNA and DNA in terrestrial insects. *Journal of Insect Science*, *3*, 1–7.

Lampert, W., & Sommer, U. (2007). *Limnoecology: The ecology of lakes and streams*. Oxford University Press.

Leonardos, N., & Geider, R. J. (2004). Responses of elemental and biochemical composition of *Chaetoceros muelleri* to growth under varying light and nitrate : Phosphate supply ratios and their influence on critical N: P. *Limnology and Oceanography*, *49*, 2105–2114.

Lewitus, A. J., & Caron, D. A. (1990). Relative effects of nitrogen or phosphorus depletion and light intensity on the pigmentation, chemical composition, and volume of *Pyrenomonas salina* (Cryptophyceae). *Marine Ecology Progress Series*, *61*, 171–181.

Lu, Y., Ludsin, S. A., Fanslow, D. L., & Pothoven, S. A. (2008). Comparison of three microquantity techniques for measuring total lipids in fish. *Canadian Journal of Fisheries and Aquatic Sciences*, *65*, 2233–2241.

Martiny, A. C., Pham, C. T. A., Primeau, F. W., Vrugt, J. A., Moore, J. K., Levin, S. A., & Lomas, M. W. (2013). Strong latitudinal patterns in the elemental ratios of marine plankton and organic matter. *Nature Geoscience*, *6*, 279–283.

Mei, Z.-P., Finkel, Z. V., & Irwin, A. J. (2009). Light and nutrient availability affect the size-scaling of growth in phytoplankton. *Journal of Theoretical Biology*, *259*, 582–588.

Melack, J. M. (2016). Aquatic ecosystems. In L. Nagy, B. R. Forsberg, & P. Artaxo (Eds.), *Interactions between biosphere, atmosphere and human land use in the Amazon Basin* (pp. 119–148). Springer.

Morales-Sánchez, D., Schulze, P. S. C., Kiron, V., & Wijffels, R. H. (2020). Production of carbohydrates, lipids and polyunsaturated fatty acids (PUFA) by the polar marine microalga *Chlamydomonas malina* RCC2488. *Algal Research*, *50*, 102016.

Novick, A., & Szilard, L. (1950). Description of the chemostat. *Science*, *112*(2920), 715–716.

Nozaki, H. (2015). Flagellated green algae. In J. D. Wehr, R. G. Sheath (Eds.), *Freshwater Algae of North America* (p. 225–252). Academic Press.

Pasciak, W. J., & Gavis, J. (1974). Transport limitation of nutrient uptake in phytoplankton. *Limnology and Oceanography*, *19*, 881–888.

Peñuelas, J., Poulter, B., Sardans, J., Ciais, P., van der Velde, M., Bopp, L., Boucher, O., Godderis, Y., Hinsinger, P., Llusia, J., Nardin, E., Vicca, S., Obersteiner, M., & Janssens, I. A. (2013). Human-induced nitrogen–phosphorus imbalances alter natural and managed ecosystems across the globe. *Nature Communications*, *4*, 2934.

Pigliucci, M. (2006). Phenotypic plasticity and evolution by genetic assimilation. *Journal of Experimental Biology.*, *209*, 2362–2367.

Plouviez, M., Bolot, P., Shilton, A., & Guieysse, B. (2023). Phosphorus uptake and accumulation in *Chlamydomonas reinhardtii*: Influence of biomass concentration, phosphate concentration, phosphorus depletion time, and light supply. *Algal Research*, *71*, 103085.

Plouviez, M., Oliveira Da Rocha, C. S., & Guieysse, B. (2022). Intracellular polyphosphate is a P reserve in *Chlamydomonas reinhardtii*. *Algal Research*, *66*, 102779.

Raven, J. A. (1984). A cost-benefit analysis of photon absorption by photosynthetic unicells. *The New Phytologist*, *98*, 593–625.

Rhee, G.-Y. (1978). Effects of N:P atomic ratios and nitrate limitation on algal growth, cell composition, and nitrate uptake. *Limnology and Oceanography*, *23*, 10–25.

Sardans, J., Rivas-Ubach, A., & Peñuelas, J. (2012). The C:N:P stoichiometry of organisms and ecosystems in a changing world: A review and perspectives. *Perspectives in Plant Ecology, Evolution and Systematics*, *14*, 33–47.

Scaife, M. A., Nguyen, G. T. D. T., Rico, J., Lambert, D., Helliwell, K. E., & Smith, A. G. (2015). Establishing *Chlamydomonas reinhardtii* as an industrial biotechnology host. *The Plant Journal*, *82*, 532–546.

Schlesinger, D. A., Molot, L. A., & Shuter, B. J. (1981). Specific growth rates of freshwater algae in relation to cell size and light intensity. *Canadian Journal of Fisheries and Aquatic Sciences*, *38*, 1052–1058.

Smith, H. L., & Waltman, P. (1995). *The theory of the chemostat: Dynamics of microbial competition*. Cambridge University Press.

Solovchenko, A. E., Ismagulova, T. T., Lukyanov, A. A., Vasilieva, S. G., Konyukhov, I. V., Pogosyan, S. I., Lobakova, E. S., & Gorelova, O. A. (2019). Luxury phosphorus uptake in microalgae. *Journal of Applied Phycology*, *31*, 2755–2770.

Sterner, R. W., & Elser, J. J. (2002). *Ecological stoichiometry: The biology of elements from molecules to the biosphere*. Princeton University Press.

Sterner, R. W., Elser, J. J., & Hessen, D. O. (1992). Stoichiometric relationships among producers, consumers and nutrient cycling in pelagic ecosystems. *Biogeochemistry*, *17*, 49–67.

Taipale, S. J., Peltomaa, E., Hiltunen, M., Jones, R. I., Hahn, M. W., Biasi, C., & Brett, M. T. (2015). Inferring phytoplankton, terrestrial plant and bacteria bulk δ^{13}C values from compound specific analyses of lipids and fatty acids. *PLoS ONE*, *10*, e0133974.

Tanioka, T., & Matsumoto, K. (2020). A meta-analysis on environmental drivers of marine phytoplankton C:N:P. *Biogeosciences*, *17*, 2939–2954.

Thrane, J., Hessen, D. O., & Andersen, T. (2016). The impact of irradiance on optimal and cellular nitrogen to phosphorus ratios in phytoplankton. *Ecology Letters*, *19*, 880–888.

Thrane, J., Hessen, D. O., & Andersen, T. (2017). Plasticity in algal stoichiometry: Experimental evidence of a temperature-induced shift in optimal supply N:P ratio. *Limnology and Oceanography*, *62*, 1346–1354.

Van Wychen, S., & Laurens, L. M. L. (2016). Determination of total carbohydrates in algal biomass: Laboratory analytical procedure (LAP). No. NREL/TP-5100-60957, 1118073. https://www.nrel.gov/docs/fy16osti/60957.pdf

Van Wychen, S., Long, W., Black, S. K., & Laurens, L. M. L. (2017). MBTH: A novel approach to rapid, spectrophotometric quantitation of total algal carbohydrates. *Analytical Biochemistry*, *518*, 90–93.

Vitousek, P. M., Aber, J. D., Howarth, R. W., Likens, G. E., Matson, P. A., Schindler, D. W., Schlesinger, W. H., & Tilman, D. G. (1997). Human alterations of the global nitrogen cycle: Sources and consequences. *Ecological Applications*, *7*, 737–750.

Wagner, N. D., Lankadurai, B. P., Simpson, M. J., Simpson, A. J., & Frost, P. C. (2015). Metabolomic differentiation of nutritional stress in an aquatic invertebrate. *Physiological and Biochemical Zoology*, *88*, 43–52.

Weers, P. M., & Gulati, R. D. (1997). Growth and reproduction of *Daphnia galeata* in response to changes in fatty acids, phosphorus, and nitrogen in *Chlamydomonas reinhardtii*. *Limnology and Oceanography*, *42*, 1584–1589.

Werner, T. P., Amrhein, N., & Freimoser, F. M. (2007). Inorganic polyphosphate occurs in the cell wall of *Chlamydomonas reinhardtii* and accumulates during cytokinesis. *BMC Plant Biology*, *7*, 51.

West-Eberhard, M. J. (2003). *Developmental plasticity and evolution*. Oxford University Press.

Zhu, S., Wang, Y., Xu, J., Shang, C., Wang, Z., Xu, J., & Yuan, Z. (2015). Luxury uptake of phosphorus changes the accumulation of starch and lipid in *Chlorella sp*. under nitrogen depletion. *Bioresource Technology*, *198*, 165–171.

SUPPORTING INFORMATION

Additional supporting information can be found online in the Supporting Information section at the end of this article.

File S1.
File S2.
File S3.
File S4.

How to cite this article: Isanta-Navarro, J., Peoples, L. M., Bras, B., Church, M. J., & Elser, J. J. (2024). Elemental and macromolecular plasticity of *Chlamydomonas reinhardtii* (Chlorophyta) in response to resource limitation and growth rate. *Journal of Phycology*, *60*, 418–431. https://doi.org/10.1111/jpy.13417